Experimentation and numerical simulation of steel fibre reinforced concrete pipes

Albert de la Fuente,[a,*] **Antonio Domingues de Figueiredo**[b], **Antonio Aguado**[a], **Climent Molins**[a] and **Pedro Jorge Chama Neto**[b]

[a] Departament d'Enginyeria de la Construcció, Universitat Politécnica de Catalunya, UPC. C/Jordi Girona 1-3, 08034 Barcelona, Spain.

[b] Departamento de Engenharia de Construção Civil, Escola Politécnica, USP. Av. Professor Almeida Prado, Trav. 2, Ed. Engenharia Civil Cidade Universtária, Brazil.

* Corresponding author: albert.de.la.fuente@upc.edu.

RESUMEN

Experimentación y simulación numérica de tubos de hormigón con fibras

Se presentan los resultados de un estudio experimental y numérico del comportamiento de tubos hormigón reforzado con fibras de acero (THFA). Se fabricaron y ensayaron en la prensa de aplastamiento 18 tubos de 600 mm de diámetro con cuantías de 10, 20 y 40 kg/m^3 de fibras. Por otra parte, se ha desarrollado un modelo numérico parametrizado para simular el comportamiento resistente de THFA sometidos al ensayo de aplastamiento, habiéndose contrastado los resultados experimentales con los obtenidos numéricamente. Los resultados han sido satisfactorios, permitiendo concluir que el modelo es útil para el diseño óptimo de este tipo de tubos y, por lo tanto, que su uso evitaría tener que recurrir al ensayo como método de diseño. En definitiva, conduciría a una reducción del coste global de estos tubos y daría un impulso al uso de fibras como elemento de refuerzo en esta tipología estructural.

PALABRAS–CLAVE: Acero, refuerzo de fibras, modelización, resistencia a flexión, caracterización

SUMMARY

Experimentation and numerical simulation of steel fibre reinforced concrete pipes

The results concerning on an experimental and a numerical study related to SFRCP are presented. Eighteen pipes with an internal diameter of 600 mm and fibre dosages of 10, 20 and 40 kg/m^3 were manufactured and tested. Some technological aspects were concluded. Likewise, a numerical parameterized model was implemented. With this model, the simulation of the resistant behaviour of SFRCP can be performed. In this sense, the results experimentally obtained were contrasted with those suggested by means MAP reaching very satisfactory correlations. Taking it into account, it could be said that the numerical model is a useful tool for the optimal design of the SFRCP fibre dosages, avoiding the need of the systematic employment of the test as an indirect design method. Consequently, the use of this model would reduce the overall cost of the pipes and would give fibres a boost as a solution for this structural typology.

KEY–WORDS: Steel, fibre reinforcement, simulation, flexural strength, characterization.

1. INTRODUCTION

Steel bar reinforced concrete pipes (SBRCP) and steel fibre reinforced concrete pipes (SFRCP) are well-known alternatives used for the conveyance of water, industrial wastes, sewerage among other applications (1-4). The addition of fibres to these pipes leads to the improvement of mechanical properties of concrete (5), as well as to economic savings (2). When steel rebars are also used, they perform the main resistance task (6), whereas the fibres activate a bridging mechanism between the cracks which leads to a reduction of their separation and opening (7). From an economic point of view, the saving of the traditional reinforcement results in a reduction of assembling operations, labour force and machinery, as well as in a decrease in the risks associated to manufacturing (2).

The use of fibres as reinforcement of concrete pipes (CP) is not a recent practice; in fact, its development began practically two decades ago. Nevertheless, its introduction into the market has been progressive, due to factors such as the risk of cuts during the manipulation tasks, lack of knowledge on design and calculation methods and, finally, the traditional inertia towards change (8).

However, through the years, solutions have been found for most of the problems previously mentioned: application of polishing so as to eliminate imperfections and avoid damages, constitutive equations to consider the tensile strength contribution of fibres in the concrete matrix (9-11) and, furthermore, it has been proved that the addition of fibres improves the mechanical behaviour of the pipe and leads to a global reduction of the costs (2 and 8).

With the purpose of examining technological and simulation aspects in detail, several experimental campaigns have been developed between the University of São Paulo (4 and 12) and the Polytechnic University of Catalonia (2). As regards the former, the work carried put concerns the procedure to follow to implement the crushing test (CT) in accordance with (13). In this sense, it was also corroborated that the continuous test is representative of the post-failure behaviour of the SFRCP, as was verified in (3). Likewise, the influence of measuring in only one of the ends of the pipe or in both ends during the execution of the CT in the results was also analyzed. Simultaneously, the Model for the Analysis of Pipes (MAP) was developed for the simulation of the mechanical response of plain concrete pipes (PCP), SBRCP, and SFRCP. This

model aims, on the one hand, at contrasting the experimental results with those derived from the model and, on the other hand, at providing a numerical tool that enables the design of the optimal reinforcement for this type of pipes.

Summarizing, the goal of this article consists in introducing the experimental campaign carried out with pipes with an internal diameter of 600 mm and C_f of 10, 20 and 40 kg/m^3, mentioning the bases of the MAP model, and contrasting the numerical results with the experimental ones in order to assess the suitability of the model as a tool for the optimal design of SFRCP.

2. PRODUCING PIPES

For the experimental campaign, a total of 18 SFRCP with a D_i of 600 mm and a h of 72 mm were manufactured, in two different series. The values of C_f used were 10, 20 and 40 kg/m^3, and 3 pipes were manufactured with each of the amounts.

In order to avoid the influence of the temporal variable, the pipes corresponding to each of the two series were manufactured on the same day, using in all cases the usual cement and aggregates at the manufacturing plant where they were produced (see Table 1). DRAMIX® RC-80/60-BN metallic fibres were used. In the 1st series there were some problems during the mixing and pouring, due to the loss of workability triggered by the addition of fibres (14). These problems were corrected in the 2nd series increasing the water content with the increase of C_f. In this way, an excellent finish level and a higher production speed were achieved.

The fibres were added directly in the conveyor belt and the concrete was compacted by means of the vibrocompression method (2). The pipes were subsequently transported and stored at the stocking area of the factory until the test date (28 days).

3. CRUSHING TEST FOR SFRCP

3.1. Procedure according to UNE-EN 1916:2002

The CT (see Fig. 1) consists in the application of a longitudinal load distributed uniformly over the upper generatrix of the pipe, which is supported on two edges forming an angle with value 2β with regard to

the centre of the pipe (O). The procedure to follow for the execution of the CT for SFRCP is specified in (15):

1. Withstanding load F_c for a minute without cracking, or in other words: without reaching load F_{cr}, F_c being equal or higher than the 67% of load F_n.
2. Leading the pipe to failure, obtaining load F_u (higher than F_n).
3. Unloading and reloading the pipe when the load decreases a 5% of F_u, verifying that a load $F_{min,pos}$ not lower than the 67% of F_n is reached. This must be maintained at least for a minute.

The intention of the cyclical process is verifying that the fibre-concrete anchorage and the post-cracking strength of SFRC are suitable for guaranteeing $F_{min,pos}$, even though it was already proved in (3) that the continuous test leads to representative and reliable results of the resistance response of the pipe.

3.2. Measuring procedure

In order to carry out the tests with enough accuracy, it was necessary to use a device that enables the uninterrupted measurement of v (12). LVDTs were used: they were stuck to the internal face of the key of the pipe and fixed in the invert. They transferred the data to a computer which processed them to obtain the F–v curves.

For the measurement of v, two configurations were used (1st series and 2nd series). In the 1st series, v was measured in the two edges of the pipe (sections A and B in Fig. 1b), the average value being the resulting displacement adopted; whereas in the 2nd series v was only measured in section A (see Fig. 1b).

4. EXPERIMENTAL RESULTS

Fig. 2 shows the average of the F–v curves for each C_f obtained in the two series (values of v up to 4 mm for pipes from the 1st series and up to 8 mm for those from the 2nd series). The F-v curves from each individual test are presented and analyzed in the experimental-numerical contrasting section.

As it can be observed, Fig. 2 shows a well-defined softening behaviour pattern in the case of pipes with low amounts of fibres; in other words, the pipe undergoes a loss of resistance capacity with the increase of v

once load F_u was reached. On the other hand, the pipes with 40 kg/m^3 respond differently, showing hardening when the yielding point is reached (points Y and Y* from Fig. 2 for the pipes with 40 kg/m^3 from the 1st and 2nd series, respectively). Consequently, the v required in order to detect the decrease of F which indicates the failure of the element and the post-failure regime are not reached in this sort of pipes.

From Fig. 2 it is also deduced that the pipes in the 1st series show higher stiffness and a longer uncracked stage. This happens because section B (Fig. 1b) is stiffer than section A (Fig. 1b) due to the higher volume of concrete involved and to the higher D_i of the former. Therefore, taking into account that the average value of v is accepted for the pipes of the 1st series, it is reasonable they show higher stiffness in comparison to those from the 2nd series, for which v was only measured in section A.

With respect to this aspect, it was observed that cracking began, in all cases, at the key of section A with values of F_{cr} around 90 kN. On the other hand, in the pipes from the 2nd series, it was observed that the appearance of the first cracks coincided with the change in the slope of the F-v curve. This change was not detected in the pipes from the 1st series until the springline also cracked, a situation which took place when load F reached average values of 126 kN, 114 kN and 138 kN for the pipes with 10 kg/m^3, 20 kg/m^3 and 40 kg/m^3, respectively. Therefore, it may be assured that if the measurement of v is performed in section A, load F_{cr} can be deduced from the F-v curve at the point where the first slope change takes place. On the other hand, if the measurement is performed as in the 1st series, this procedure would lead to values of F_{cr} on the side of insecurity, requiring a visual inspection in order to detect F_{cr}.

In the case of the pipes with low C_f, instability regions similar to those described in (3) were observed. They were reflected in the F-v curves by means of an increase in the distance between points (see, for instance, the stretch between 1.5 and 3.0 mm of the pipes with 20 kg/m^3 from the 2nd series).

Likewise, it was verified that the pipes fulfilled the strength requirements of class C-90 established in (15). Concretely, for pipes with a D_i of 600 mm it is required to obtain a load F_c of 36 kN/m and a load F_u of 54 kN/m in the CT (90 kN and 135 kN, respectively, taking into account that the length of the pipes was 2500 mm).

Regarding load $F_{min,pos}$, established for C-90 (90 kN), it must be verified that the $F_{max,pos}$ measured in the curve F-v is equal or higher than the former. The value of v for which $F_{max,pos}$ is reached is function of, among other parameters, the diameter of the pipe and the amount and type of reinforcement; in other words,

of the global stiffness of the pipe. For this paper it was established that $F_{max,pos}$ is reached for a v of 1.2 mm ($F_{1.2mm}$) and 3 mm (F_{3mm}) for the pipes from the 1st and the 2nd series, respectively (3). However, this is not the suitable approach in the case of pipes with 40 kg/m^3, since they did not show a drop of value F for the displacement regime used in the tests. Consequently, in the case of those pipes only their load F_u is assessed, and it is taken for granted that their post-failure behaviour fits in with the criteria established for class C-90 (the pipes with 20 kg/m^3 already fulfil the minimum requirements in post-failure regime).

Table 2 shows the individual and average values of F_{cr}, $F_{1.2mm}$ (1st series), F_{3mm} (2nd series) and F_u obtained experimentally. The results from pipes T3 for the amounts of 10 kg/m^3 and 20 kg/m^3 from the 1st series were rejected due to some mismatches which occurred during the performance of the test.

Concerning the values gathered in Table 2, it is deduced that the pipes from the 1st series showed loads F_{cr} higher than the 90 kN stipulated for F_c in C-90. Likewise, the pipes from the 2nd series showed average loads of F_{cr} around 94 kN, which were also accepted since no cracking signs were observed during the visual inspection once F_c was reached, not even in pipes T1 and T2 with amounts of 40 kg/m^3 from the 2nd series, for which the load F_{cr} was 80 kN.

As regards the response in failure, the values F_u were obtained for displacements close to 0.3 mm for the pipes from the 1st series and close to 1 mm for those from the 2nd series, thus corroborating the stiffer behaviour of the former. It is deduced from Table 2 that, in average value, all the pipes reached the load of 135 kN established for F_u except the pipes reinforced with 20 kg/m^3 and 10 kg/m^3 of fibres from the 1st series and the 2nd series, respectively. In both cases the average load F_u obtained was of 132 kN (a 2% lower than required). Finally, it is verified that load $F_{min,pos}$ (90 kN) is exceeded by all the pipes except pipe T2 with 10 kg/m^3 of fibres from the 2nd series. In any case, the average values of $F_{1.2mm}$ and F_{3mm} are higher than the $F_{min,pos}$ established for these pipes, proving that the type of fibres and the amounts used are the suitable ones to accomplish the strength requirements.

5. NUMERICAL SIMULATION OF CRUSHING TEST

The numerical simulation of the CT requires a numerical tool capable to consider the nonlinear behaviour of the material and the possibility of modelling the response of SFRC. To this purpose, the Analysis of Evolutive Sections model (AES), described in (16 and 17), was used. This model has already

been used satisfactorily as a numerical tool in other applications (18). On the other hand, the MAP model was developed for the simulation of the CT. Several of the hypotheses accepted in the MAP model were suggested in (19).

By means of the AES model the concrete is discretized into fibre-type elements and the steel bars, into concentrated area elements. It is well known that the addition of fibres modifies the compression behaviour of SFRC depending on the volume used (20). In this respect, its response to uniaxial compression is described by the expression suggested in (21). On the other hand, the simulation of its post-cracking behaviour is approached by means of the model gathered in (11), since it has already been successfully used in other works (22 and 23). The passive steel for the reinforcement is modelled using a trilinear diagram.

For the simulation of the CT at a structural level, the double symmetry of the element (β=0) was taken into account, hence only a quarter of pipe is modelled. Likewise, it is taken for granted that the key and springline sections are the ones which control the response of the pipe. The cracking and yielding phenomena (modelled with the AES subroutine) are concentrated in both sections, whereas in the intermediate sections a linear behaviour of the constituting materials is accepted. The response of the pipe has been divided into three stages: elastic linear stage, elastic stage with cracking at key (see Fig. 1) and elastic stage with cracking at key and springline (see Fig. 1).

The governing equations of the structural problem implemented in MAP were deduced in (19) considering that the bending and axial forces are the determinant ones. In this respect, it is well known that the shear strength of SFRC elements improves noticeably (24), so shear failures are not expected in this type of pipes.

Taking into account the three stages previously described, the curve ***F-v*** of the pipe in the CT can be obtained. However, the model guarantees representative results of the CT, provided that no intermediate cracks appear (rigid concrete pipes). This is the pattern observed in the pipes tested for this campaign. Likewise, it has also been observed in SFRCP with D_i of 800 mm (3) and of 1000 mm (2), hence the latter is established as the maximum value of the applicability range of the model for lack of contrasting with larger diameters.

6. SIMULATIONS OF THE EXPERIMENTAL RESULTS WITH MAP

The model suggested in (21) was used for modelling the compression behaviour of SFRC, fixing a resistance f_{ck} of 50 MPa (4). On the other hand, the diagram proposed in (11) was used in order to simulate its linear and post-cracking response. However, due to the lack of tests needed (25) in order to be able to determine $f_{R,i}$ for each C_f, the expressions proposed in (26) were used. In this respect, the type of fibres used in this campaign as well as those used in order to calibrate the expressions presented in (26) belong to the type DRAMIX® RC-80/60-BN.

Figs. 3 show the curves F-v obtained experimentally (individual and average values) and numerically for the pipes with C_f of 10, 20 and 40 kg/m^3 from the 2nd series. This series was selected because it was observed that the experimental measurements of v in section A (Fig. 1b) are more representative of the global behaviour of the pipe.

Complementarily, Table 3 gathers the average experimental and numerical values of F_c, F_u and F_{3mm} shown in Figs. 3. The parameter ξ is the relative error with regard to the experimental data. Positive values of ξ indicate that the experimental data exceed the numerical one, and vice versa.

From the results presented in Fig. 3a, it can be deduced that the MAP model fits in properly with the experimental results for the amount of 10 kg/m^3, particularly both in elastic linear and post-failure stages. In the latter, the numerical results for v higher than 7.5 mm tend toward the experimental maximum values. The values of F_{cr}, F_u and F_{3mm} obtained numerically are 98 kN, 114 kN and 88 kN, respectively. Therefore, since neither F_u nor F_{3mm} reach the minimum values stipulated in (15) for class C-90, it can be stated that according to the model the amount of 10 kg/m^3 is not enough to guarantee strength class C-90.

The results from Fig. 3b concerning the dosage of 20 kg/m^3 highlight that the simulation by means of the MAP model guarantees values close to the experimental ones. Nonetheless, the model overestimates the load capacity of the pipes for v higher than 5.5 mm. This could indicate that the values $f_{R,i}$ used for the simulation of the behaviour of tensioned SFRC are slightly higher than the real ones for this range of displacements. The values of F_{cr}, F_u and F_{3mm} obtained numerically are: 98 kN, 123 kN and 108 kN, respectively. Consequently, class C-90 will not be reached with 20 kg/m^3 either, since the load F_u (123 kN) is lower than the 135 kN required.

Finally, in the case of the pipes with 40 kg/m^3 of fibres (Fig. 3c), the numerical model fits in adequately with the experimental results at all stages. In this case, the value of F_{cr} is 98 kN and F_u is 156 kN. Therefore, the model also predicts a strength capacity higher than that specified for a class C-90 pipe of 600 mm (15) with this amount of fibres. In this respect, it is taken for granted that the load F_{3mm} is higher than the 90 kN established for $F_{min,pos}$ (with 20 kg/m^3, the average F_{3mm} is already 108 kN). Likewise, the model highlights, in accordance with the experimental results, the existence of hardening once the pipe yields.

From the analysis of the results presented in Table 3 it can be concluded that:

- The load F_{cr} obtained numerically is independent from the amount of fibres. F_{cr} depends exclusively on f_{ct}, D_i and h (2). On the other hand, the model tends to overestimate F_{cr} with respect to the experimental results between a 4.3% (pipe with 10 kg/m^3) and a 6.5% (pipe with 40 kg/m^3). This could be due to the incorporation of additional water during the mixing in order to increase the workability of the mixture in the pipes from the 2nd series.
- The model underestimates F_u with regard to the experimental values between a 3.7% (pipe with 40 kg/m^3) and a 13.6% (pipe with 10 kg/m^3). When F_u is reached, then the reason for the difference obtained could be the constitutive equation used to simulate the post-cracking behaviour of SFRC being too conservative for the levels of v at which F_u is reached. In this respect, in (2) it is verified that the fibres work practically oriented parallel to the flow of stresses when the conventional pipe manufacturing methods are used. Therefore, they work with a high efficiency. An alternative way of considering this fact at the level of calculation would be using the methodology suggested in (27), for example.
- With regard to F_{3mm}, the numerical values obtained are a 6.4% (10 kg/m^3) and a 6.9% (20 kg/m^3) lower in comparison with the experimental data. This could be due, just as in the case of load F_u, to the underestimation of the parameters involved in the definition of the constitutive equation chosen (11) to model the post-cracking response of SFRC.

Taking into account what has been previously mentioned, it can be assured that the MAP model adjusts satisfactorily to the experimental results, even though a constitutive equation was used in order to model the post-cracking behaviour of SFRC, calibrated from concretes with f_{ck} ranging from 25 to 30 MPa (26) as

opposed to the 50 MPa obtained in the concrete used for the pipes in this campaign. Likewise, the constitutive equation does not take into account the effect of the preferential orientation of the fibres within the thickness of the pipe, which in this case is favourable. Consequently, in most of the cases the MAP model tends to underestimate the experimental results, these differences being of a 7.0% in average value and, in any case, not higher than 13.6%. Then, the good correlation obtained can be considered to be a success taking into account the multitude of variables involved in the problem, its uncertainty, and the difficulty of the experimental determination of some of them.

7. CONCLUSIONS

This article has introduced a work related to the technological aspects and the numerical simulation of SFRCP. It also showed the results obtained in an experimental campaign with 18 SFRC pipes with diameters of 600 mm and amounts of fibres of 10, 20 and 40 kg/m^3. The following conclusions were derived from those results:

- The manufacturing of this type of elements is possible by means of the traditional systems modifying *in situ*, if necessary, the water content of the mixture. The manufacturing time and the labour force are reduced considerably with respect to SBRCP.
- It is confirmed that the continuous test with displacement control by means of LVDTs, as a replacement for cyclical tests, leads to results representative of the strength capacity of this sort of pipes.
- The load $\boldsymbol{F_{cr}}$ observed during the visual inspection is similar regardless of the amount of fibres and the measuring method. The first crack appeared, in all cases, in the internal face of the key (in section A). In the case of the pipes from the 2nd series, the point where the first change in the slope of curve ***F-v*** occurs coincides with $\boldsymbol{F_{cr}}$, exactly as in the numerical simulations.
- The pipes with 40 kg/m^3 show hardening of the curve ***F-v*** when global cracking of the pipe (key and springline) occurs. From this fact it is deduced that in these elements the fibres can perform a task similar to that of the traditional bars, even with an improved response to cracking in in-service regime
- The load which is critical in order to fulfil the strength requirements of class C-90 for this type of pipes is $\boldsymbol{F_u}$.

Moreover, the main bases of the MAP model, developed for the analysis of SFRCP, were introduced. The degree of correlation between experimentation and simulation is considered to be satisfactory, since the model gave results on the side of security with an average relative error of 7.0%. In order to improve the accuracy of the results, it is proposed to adjust the constitutive equation of post-cracked SFRC so that it takes into account the preferential orientation of the fibres.

Consequently, the MAP model can be used as a design method for other diameters (equal or lower than 1000 mm), other thickness and other strength classes, without the need for testing several pipes in order to estimate the optimal dosage of fibres, but only to verify the resulting design. This would mean a significant saving of time and economic resources when there is no established dosage pattern, be it because some geometrical characteristic has been changed, or because it is a strength class uncommon for such a diameter.

Currently, several experimental campaigns are being carried out with the aim of contributing to a larger data bank to contrast and adjust the model.

ACKNOWLEDGEMENTS

The authors of this document wish to express their appreciation for the financial support received through the Research Project BIA2010-17478: *Procesos constructivos mediante hormigones reforzados con fibras*.

Likewise, Professor Antonio D. de Figueiredo wishes to thank the support provided by CAPES - Coordenação de Aperfeiçoamento de Pessoal de Nível Superior– for having awarded him the postdoctoral grant that allowed him to participate in this work.

REFERENCES

(1) Haktanir T, Ari K, Altun F, Karahan O. A comparative experimental investigation of concrete, reinforced-concrete and steel-concrete pipes under three-edge-bearing test. *Construction and Building Materials* 2007; **21**(8): 1702-8. doi:10.1016/j.conbuildmat.2006.05.031.

(2) de la Fuente A, Armengou J. Aplicaciones estructurales del HRFA: Tubos de saneamiento, paneles de cerramiento y placas de suelo reforzado. *Aplicaciones estructurales del HRFA*, Jornada Técnica 2007-JT-02, 9 de Octubre de 2007, Barcelona (Spain), UPC, 2007.

(3) Figueiredo AD de. Evaluation of the test method for crushing strength of steel fiber reinforced concrete pipes. *7th International RILEM Symposium on Fibre Reinforced Concrete*, Chennai, India, 2008. Fiber Reinforced Concrete: Design and Applications. Babneux - France: RILEM Publications SARL 2008; **1**:989–1000.

(4) Figueiredo AD de, Chama Neto PJ. Avaliação de desempenho mecânico de tubos. *Revista DAE* 2008; 178: 34-9.

(5) Aa'ad S, Saxer A. Influence of Fiber Geometry on the Flexural Strength Performance of Steel Fiber Reinforced Concrete (SFRC), *Fibre Concrete 2007*, Prague, Czech Republic, 2007.

(6) Chiaia B., Fantilli AP, Vallini, P. Evaluation of crack width in FRC structures and application to tunnel linings. *RILEM Materials and Structures* 2009; **42**(3):339-51. doi:10.1617/s11527-008-9385-7.

(7) Blanco A, Pujadas P, de la Fuente A, Aguado, A. Análisis comparativo de los modelos constitutivos del hormigón reforzado con fibras. *Hormigón y Acero* 2010; 61(256):83-100.

(8) Parrot J. *Estudio de la sostenibilidad en tuberías de saneamiento*, Tesina de especialidad, UPC, Barcelona (Spain). 2009.

(9) Hilleborg A, Modéer M, Petersson PE. Analysis of crack formation and crack growth in concrte by means of fracture mechanics and finite elements. *Cement and Concrete Research* 1976; **6**:773-82.

(10) Laranjeira, F. Design-oriented constitutive model for steel fiber reinforced concrete. PhD Thesis, UPC, Barcelona (Spain), 2010.

(11) Vandewalle, L. *et al*. Test and design methods for steel fibre reinforced concrete: σ-ε design method. Final recommendation. *RILEM Materials and Structures* 2003; **36**(262):560-67. doi:10.1617/14007.

(12) Silva JL da, el Debs MK. Influência da bolsa no comportamento estrutural de tubos de concreto armado submetidos à compressão diametral. In: *51º Congresso Brasileiro do Concreto*, 2009, Curitib (Brazil). p.1-13.

(13) UNE-EN 1916:2002. *Concrete pipes and fittings, unreinforced, steel fibre and reinforced*. 2002.

(14) Moreno E, Fernández M. Mix design of steel fiber reinforced concrete. *Materiales de Construcción* 1997; **47**(247-248):11-26. doi:10.3989/mc.1997.v47.i247-248.

(15) UNE 127916. *Tubos y piezas complementarias de hormigón en masa, de hormigón con fibra de acero y de hormigón armado*. Complemento nacional a la norma UNE-EN 1916:2003. 2004.

(16) de la Fuente A, Aguado A, Molins C. Modelo numérico para el análisis no lineal de secciones prefabricadas construidas evolutivamente. *Hormigón y Acero* 2008; **57**(247):69-87.

(17) de la Fuente A, Aguado A, Molins C. Diseño óptimo integral de tubos de hormigón. *Hormigón y Acero* 2010; **61**(259). [In press].

(18) Klein N, de la Fuente A, Aguado A, Masó D. Hormigón ligero autocompactante con fibras para rehabilitación de forjados. *Materiales de Construcción*. Accepted in 2010 for publication.

(19) Pedersen EJ. *Calculation of FRC pipes based on the fictius crack model*. Department of Structural Engineering. Technical University of Denmark, 1995.

(20) Bencardino F, Rizzuti L, Spadea G, Swamy RN. Stress-strain behavior of steel fiber-reinforced concrete in compression. *ASCE Journal of Materials in Civil Enineering* 2008; **20**(3):255-63. doi:10.1061/(ASCE)0899-1561(2008)20:3(255).

(21) Barros JAO, Figueiras JA. Flexural behaviour of SFRC: Testing and modelling. *ASCE Journal of Materials in Civil Enineering* 1999; **11**(4):331-9. doi:10.1061/(ASCE)0899-1561(1999)11:4(331).

(22) Blanco A. *Durabilidad del Hormigón con Fibras de Acero*. Tesina de especialidad, UPC, Barcelona (Spain). 2008.

(23) Pujadas P. *Durabilidad del Hormigón con Fibras de Polipropileno*. Tesina de especialidad, UPC, Barcelona (Spain). 2008.

(24) Turmo, J., Banthia, N., Gettu, R., and B. Barragán. Study of the shear behaviour of fibre reinforced concrete beams. *Materiales de Construcción* 2008; **58**(292):5-13. doi:10.3989/mc.2008.40507.

(25) Vandewalle L. *et al*. Test and design methods for steel fibre reinforced concrete: Bending test (final recommendation). *RILEM Materials and Structures* 2002; **35**(253):579-82. doi:10.1617/13884.

(26) Barros JAO, Cunha VMCF, Ribeiro AF, Antunes JAB. Post-cracking behaviour of steel fibre reinforced concrete. *RILEM Materials and Structures* 2005; **38**(1):47-56. doi:10.1007/BF02480574.

(27) Laranjeira F, Molins, C, Aguado, A. Predicting the pullout reponse of inclined hooked steel fibers.

Cement and Concrete Research 2010; **40**(10):1471-87. doi:10.1016/j.cemconres.2010.05.005.

APENDIX. NOMENCLATURE

A:	Male joint member of the pipe.
B:	Female joint member of the pipe.
C_f:	Fibre dosage.
D_i:	Internal diameter of the pipe.
D_o:	Outside diameter of the pipe.
d_{max}:	Maximum diameter of the aggregate.
E_{cm}:	Average elongation modulus of the concrete.
F:	Applied load.
F_c:	Service load (established).
F_{cr}:	First cracking load.
F_n:	Failure load (established).
$F_{max,pos}$:	Maximum post-failure load (simulated).
$F_{min,pos}$:	Minimum post-failure load (established).
F_u:	Failure load.
$F_{1.2mm}$:	Post-failure load for a 1.2 mm vertical displacement of the key (1st series).
$F_{3.0mm}$:	Post-failure load for a 3.0 mm vertical displacement of the key (2st series).
f_{ck}:	Characteristic compressive concrete strength.
f_{ct}:	Tensile concrete strength.
f_{Ri}:	Residual flexural concrete strength.
h:	Thickness of the concrete wall.
l:	Length of the pipe.
O:	Centre of the pipe.
v:	Vertical displacement of the key.
β:	Angle between the supports and the centre of the pipe.
ξ:	Relative error of the numerical value.

TABLES

Table 1

Dosages used for manufacturing the SFRCP

Material	Dosage
River Sand (d_{max} = 1.2 mm)	679 kg/m^3
Crushed Sand (d_{max} = 4.8 mm)	340 kg/m^3
Granitic Crushed Coarse Aggregate (d_{max} = 9.5)	1067 kg/m^3
Cement	355 kg/m^3
Water	152 l/m^3
Fibres	10, 20 y 40 kg/m^3

Table 2

Individual and average values of *F* experimentally obtained.

Series	C_f **(kg/m^3)**	F_{cr} **(kN)**				F_u **(kN)**				$F_{1.2mm}$ y F_{3mm} **(kN)**			
		T1	T2	T3	**Average**	T1	T2	T3	**Average**	T1	T2	T3	**Average**
1st	10	96	98	n/a	**97**	149	120	n/a	**135**	107	94	n/a	**101**
	20	96	100	n/a	**98**	140	124	n/a	**132**	118	102	n/a	**110**
	40	93	98	100	**97**	156	163	149	**156**	-	-	-	**-**
2nd	10	100	83	100	**94**	127	132	138	**132**	97	88	98	**94**
	20	98	95	85	**93**	151	145	129	**142**	121	120	108	**116**
	40	80	80	115	**92**	152	140	193	**162**	-	-	-	**-**

Table 3

Experimental (average) and numerical values of *F* obtained with the tested pipes

Fibre dosage (kg/m^3)	F_{cr}			F_u			F_{3mm}		
	Exp. (kN)	MAP (kN)	ξ (%)	Exp. (kN)	MAP (kN)	ξ (%)	Exp. (kN)	MAP (kN)	ξ (%)
10	94	98	-4.3	132	114	13.6	94	88	6.4
20	93	98	-5.4	142	123	13.4	116	108	6.9
40	92	98	-6.5	162	156	3.7	-	-	-

FOOTNOTES OF THE FIGURES

Figure 1. (a) Cross and (b) longitudinal sections of the test configuration.

Figure 2. Average *F*-*v* curves obtained for the tested pipes.

Figure 3. *F*-*v* curves for the pipes reinforced with (a) 10, (b) 20 y (c) 40 kg/m^3 of fibres.

1 FIGURES

2 Figure 1

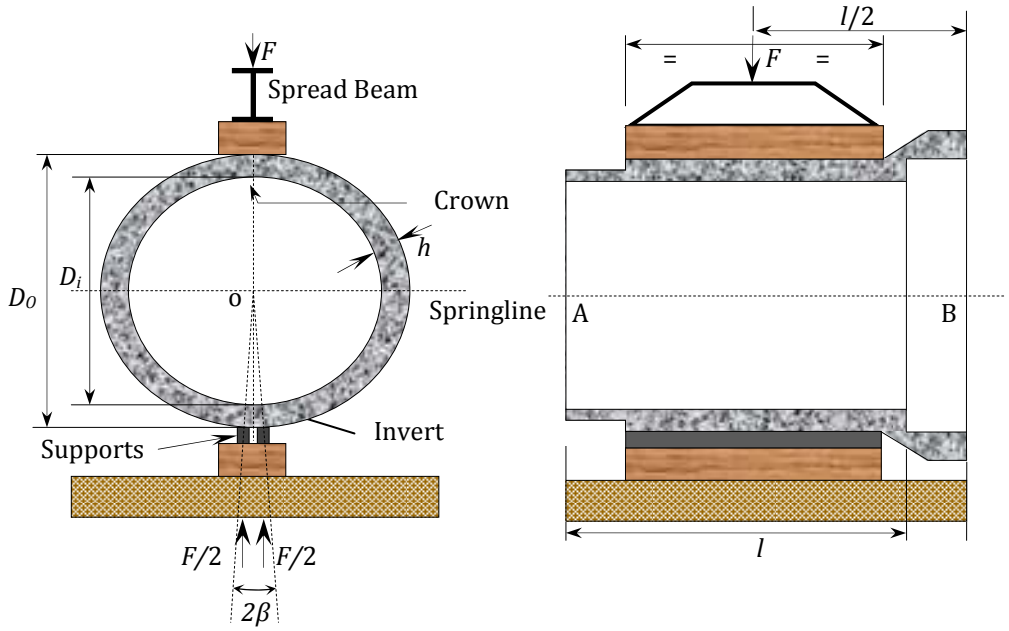

Figure 2

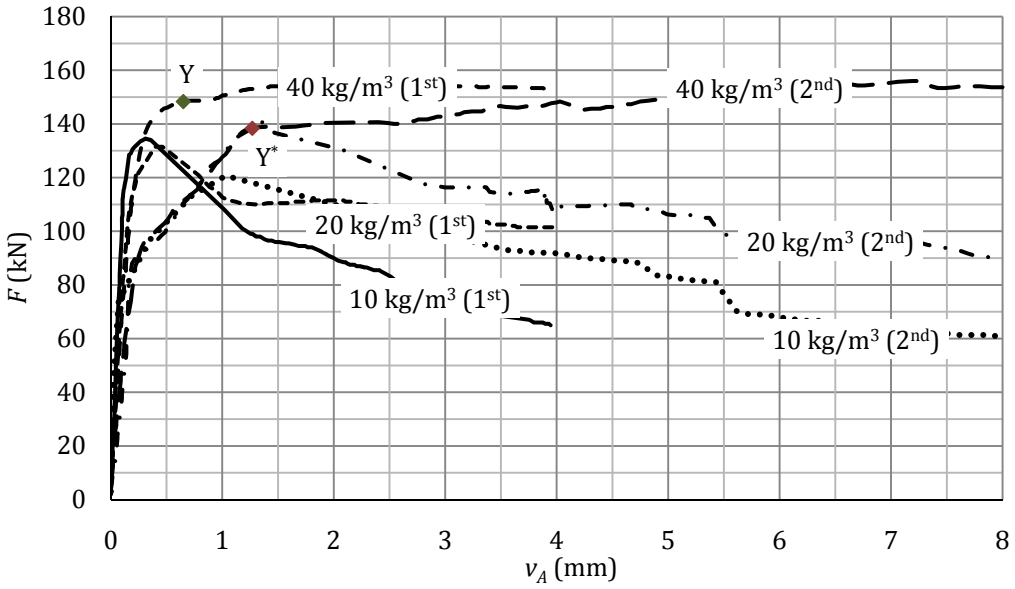
180
160
140
120
100
80
60
40
20
0
0
1
2
3
4
5
6
7
8
F (kN)
v_A (mm)
Y
Y*
40 kg/m³ (1st)
40 kg/m³ (2nd)
20 kg/m³ (1st)
20 kg/m³ (2nd)
10 kg/m³ (1st)
10 kg/m³ (2nd)

Figure 3

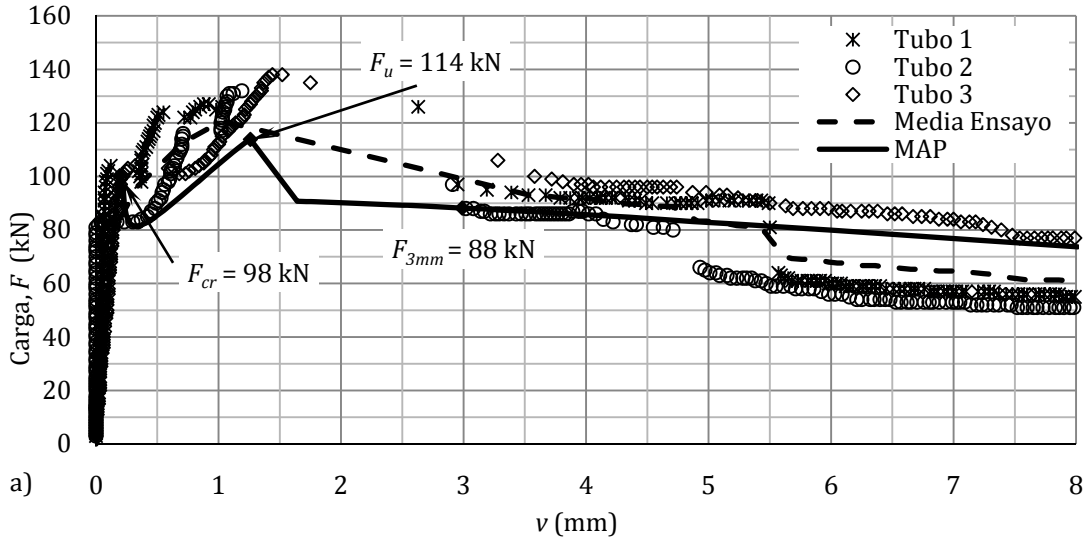
F_u = 114 kN
F_{3mm} = 88 kN
F_{cr} = 98 kN
Tubo 1
Tubo 2
Tubo 3
Media Ensayo
MAP
Carga, F (kN)
v (mm)

a)

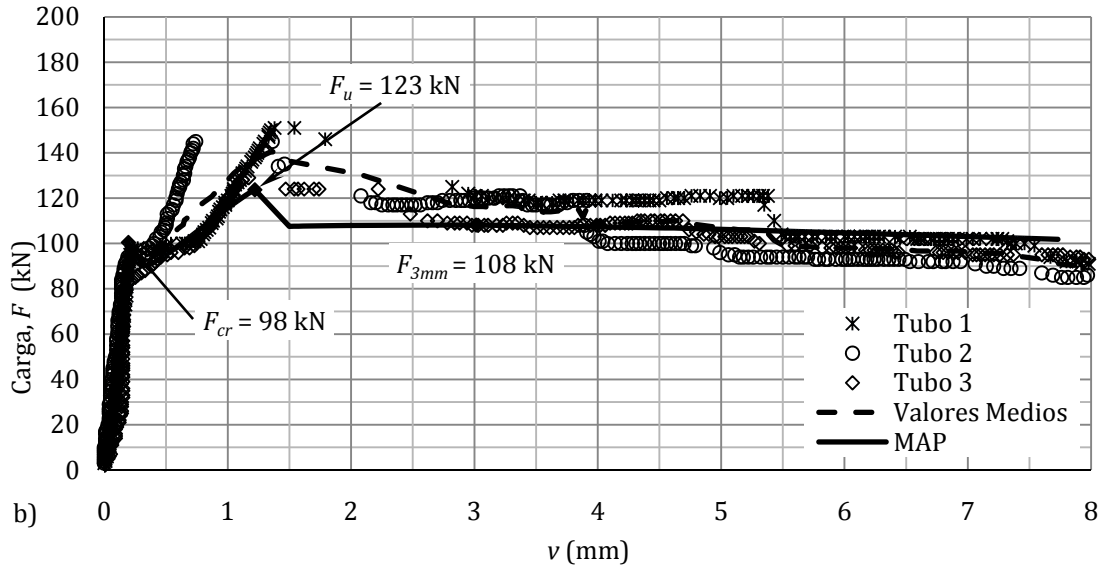
F_u = 123 kN
F_{3mm} = 108 kN
F_{cr} = 98 kN
Tubo 1
Tubo 2
Tubo 3
Valores Medios
MAP
Carga, F (kN)
v (mm)

b)

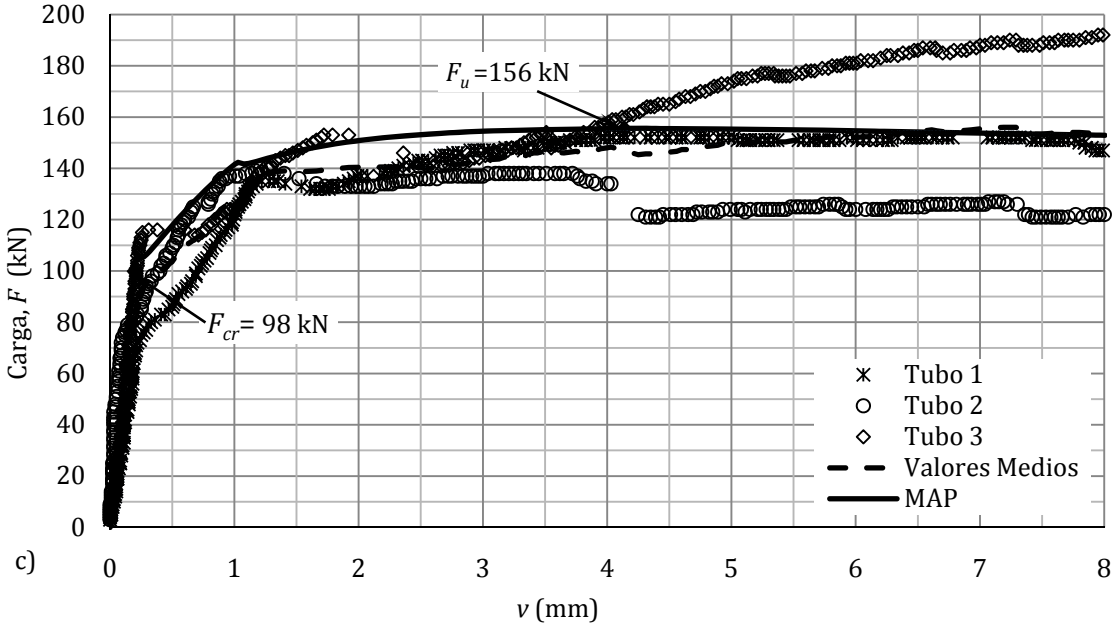
F_u =156 kN
F_{cr}= 98 kN
Tubo 1
Tubo 2
Tubo 3
Valores Medios
MAP
Carga, F (kN)
v (mm)

c)